Electronic Supplementary Information

Influence of Halide Ions on the Structure and Properties of Copper Indium Sulphide Quantum Dots

Riccardo Marin,[a,b] Artiom Skripka,[b] Yu-Cheng Huang,[c] Tamie A.J. Loh,[d] Viktoras Mazeika,[e] Vitalijus Karabanovas,[e,f] Daniel H.C. Chua,[d] Chung-Li Dong,[c] Patrizia Canton,[a] and Fiorenzo Vetrone[b]**

[a] Università Ca' Foscari Venezia, Dipartimento di Scienze Molecolari e Nanosistemi, via Torino 155/B – 30170 Venezia-Mestre (Italy)

[b] Institut National de la Recherche Scientifique (INRS), Centre Énergie, Matériaux et Télécommunications (EMT), Université du Québec, 1650 Boul. Lionel-Boulet, Varennes, QC J3X 1S2 (Canada)

[c] Department of Physics, Tamkang University, Tamsui, 25137 (Taiwan)

[d] Department of Material Science and Engineering, National University of Singapore, 9 Engineering Drive 1, 117575 (Singapore)

[e] Biomedical Physics Laboratory, National Cancer Institute, P. Baublio St. 3b, LT-08406 Vilnius (Lithuania)

[f] Department of Chemistry and Bioengineering, Vilnius Gediminas Technical University, Sauletekio Ave. 11, LT-10223 Vilnius (Lithuania)

Table of contents:

Experimental procedure.

Chemicals

Copper iodide (CuI, 99.999%), copper bromide (CuBr, 99.999%), copper chloride (CuCl, 99.999%), copper acetate (CuAc, 98%) indium acetate ($In(OAc)_3$, 99.99%) and 1-dodecanethiol (DDT, 98%) were purchased from Sigma Aldrich. 1-octadecene (ODE, 90%), oleic acid (OA, 90%), chloroform (99.8%) and hexane (99%) were obtained from Alfa Aesar. Ethanol (100%) and methanol (99.9%) were obtained from Commercial Alcohols and Fisher Scientific respectively. All chemicals were used as received.

Quantum dots synthesis

Copper indium sulphide (CIS) quantum dots (QDs) have been synthesized according to a simple thermal decomposition method.[1] The samples were named after the copper source used in the synthesis: CIS-Cl, CIS-Br, CIS-I, and CIS-ac when CuCl, CuBr, CuI, and CuAc were used respectively.

Briefly 0.2 mmol of copper(I) halide, 0.2 mmol of $In(OAc)_3$, 10 mL of ODE, 3.9 mL (16 mmol) of DDT, and 0.708 mL (2 mmol) of OA were introduced in a 50-mL three-necked round bottom flask. The solution was stirred at 100 °C under vacuum for 1 h and backfilled with Ar. Then, the temperature was raised to 120 °C and maintained at this stage for 5 min. The temperature was further raised to 150 °C and maintained for 5 min. Eventually, the temperature was set to 230 °C. Upon heating the solution became clear and slightly yellow. The colour further changed to deep yellow, orange, red, and eventually dark brown indicating the nucleation and subsequent growth of the QDs. Aliquots were taken at different time intervals after reaching 230 °C (5 min, 10 min, 20 min, 30 min, 45 min, 60 min, 90 min) and after 120 min the flask was quenched in cold water. Each aliquot (approx. 400 µL) was quenched in 100 µL of cold hexane and precipitated by the addition of 1 mL of ethanol. The QDs were centrifuged and the supernatant discarded. The nanoparticles were further dispersed in 200 µL of hexane and washed twice with ethanol, before being re-dispersed in hexane for optical characterization.

For X-Ray Photoemission Spectroscopy (XPS), Powder X-Ray Diffraction (PXRD), and Transmission Electron Microscopy (TEM) analyses, the nanoparticles were further washed thoroughly using a mixture of chloroform:methanol (1:1) to precipitate the QDs out from hexane. This process was repeated at least three times to ensure the removal of unreacted precursors. The samples were either re-dispersed in hexane or dried in air, depending on the characterization technique employed.

Optical characterization

For the optical absorption studies, the sols were diluted in hexane to an optical density below 1 throughout the whole measurement range. The spectra were acquired on a Varian Cary 5000 Spectrophotometer with a 1-nm resolution at a speed of 600 nm/min.

The photoluminescence (PL) spectra were recorded on a Varian Cary Eclipse Fluorescence Spectrophotometer equipped with a Xenon flash lamp. For the emission studies the optical density of the sol was kept below 0.1 at the excitation wavelength (455 nm). To compare the emission intensity of the samples reacted for 30 min, their optical density was adjusted to approximately 0.05 at the excitation wavelength. For the photoluminescence quantum yield (*PLQY*) determination, an aqueous $Ru(bpy)_3Cl_2$ solution was used as a standard ($PLQY_{ref}$ = 0.042 ± 0.002)[2] and the following equation was employed:

$$PLQY_{QD} = PLQY_{ref}\frac{I_{QD}}{I_{ref}}\frac{A_{ref}}{A_{QD}}\left(\frac{n_{QD}}{n_{ref}}\right)^2 \qquad 1$$

Where *I* is the integrated emission intensity, *A* is the absorbance at the excitation wavelength (420 nm), *n* is the refractive index of the solvent in which the sol (hexane for the QDs, n_{QD} = 1.375) or solution (water for the standard, n_{ref} = 1.333) are prepared. The subscripts *QD* and *ref* refer to the sample and the standard, respectively. Since the recorded emission spectra are cut at 810 nm, to obtain an estimation of the *PLQY* of the samples the peaks were fitted with two Gaussian curves and the integrated area of the fitted curves was used. This approach could (and likely does) lead to underestimation of the calculated values. However, the identical treatment of the experimental data in the three cases makes for a fair *relative* comparison between the three samples. See Figures S13 and S14 below.

Photoluminescence decay measurements were performed with a F920 spectrophotometer (Edinburgh Instruments, Livingston, UK), equipped with a single photon photomultiplier detector (S900-R – Hamamatsu, Shizuoka, Japan) and a picosecond pulsed diode laser (EPL-405) (excitation wavelength 405 nm, pulse width 66.9 ps, repetition rate 2 MHz) (Edinburgh Instruments, Livingston, UK). Quartz cuvettes with optical path length of 1 cm were used for all measurements. Decay curves were recorded at the maximum of the photoluminescence peak of each sample.

Morphological, structural and chemical characterization

The crystalline phase of the samples was investigated by means of PXRD with a Bruker D8 Advance Diffractometer using a Cu Kα radiation. The diffraction patterns were fitted *via* Rietveld refinement on the software GSAS® in order to obtain information about the lattice parameters.

The composition of the samples was investigated by means of XPS, recording the spectra with a VG ESCALAB 200i XL using an Al Kα monochromatic source. The spectra were analysed using XPSpeak41® software.

For both PXRD and XPS measurements the samples were prepared casting few drops of the hexane sols of purified QDs on a glass slide and letting the solvent evaporate in air.

The morphology of the samples was investigated by means of TEM and HRTEM (High Resolution TEM) using a JEOL JEM 3010 microscope (1.7 Å point to point resolution at Scherzer defocus). Energy Dispersive X-rays Spectroscopy (EDS) spectra were recorded using an Oxford Instruments ISIS Series 300 spectrometer. Before the imaging, each sample was further diluted in hexane to an approximate concentration of 0.1 mg/mL and sonicated for 2 min. One drop of the solution was deposited on a holey carbon-coated nickel grid and the solvent was allowed to slowly evaporate in air.

X-ray absorption spectroscopy (XAS), including X-ray absorption near edge spectroscopy (XANES) and extended X-ray absorption fine structure (EXAFS) studies, were performed at National Synchrotron Radiation Research Center (NSRRC), Hsinchu, Taiwan. Cu K-edge was carried out at BL17C. S K- and In L_3-edge were conducted at BL16A. Both measurement at BL17C and BL16A were made by transmission mode.

Additional TEM images.

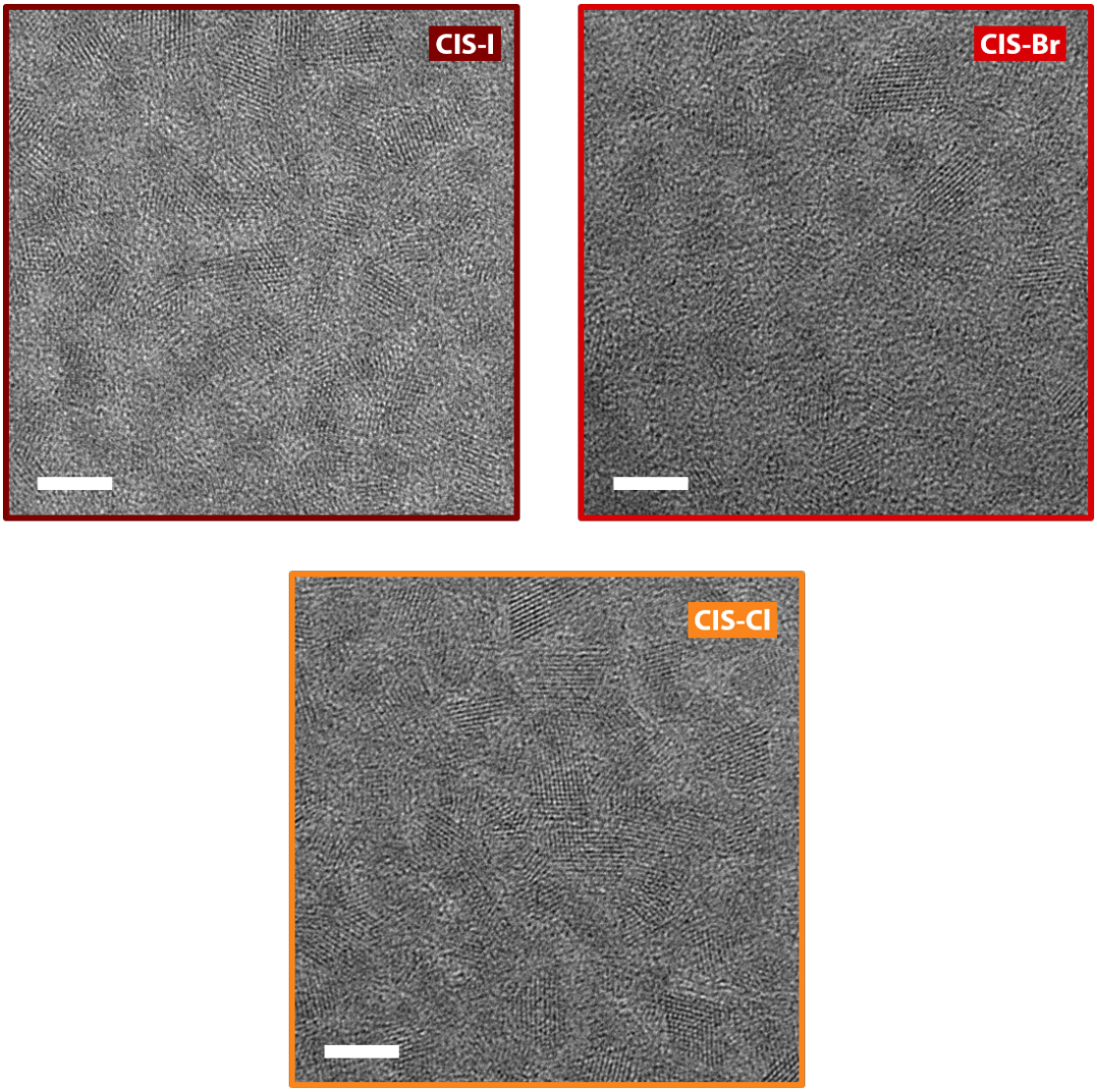

Figure S1. TEM images obtained for the three CIS-I, CIS-Br and CIS-Cl samples reacted for 120 min. Scale bars are 5 nm.

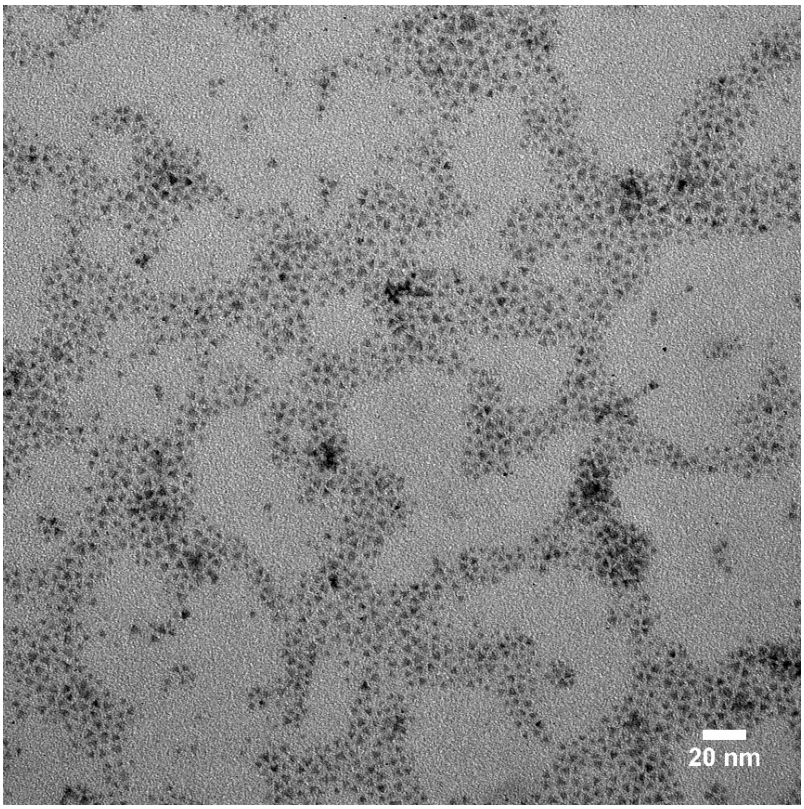

Figure S2. Additional TEM image obtained from a freshly synthesized CIS-I batch of QDs reacted for 30 min. This image was obtained on a different microscope - JEM1400 Flash (JEOL) operating at 100 kV acceleration voltage. Triangular features are clearly observable in accordance with the preferred tetrahedral shape of CIS QDs crystallized in the chalcopyrite polymorph.

EDS spectra.

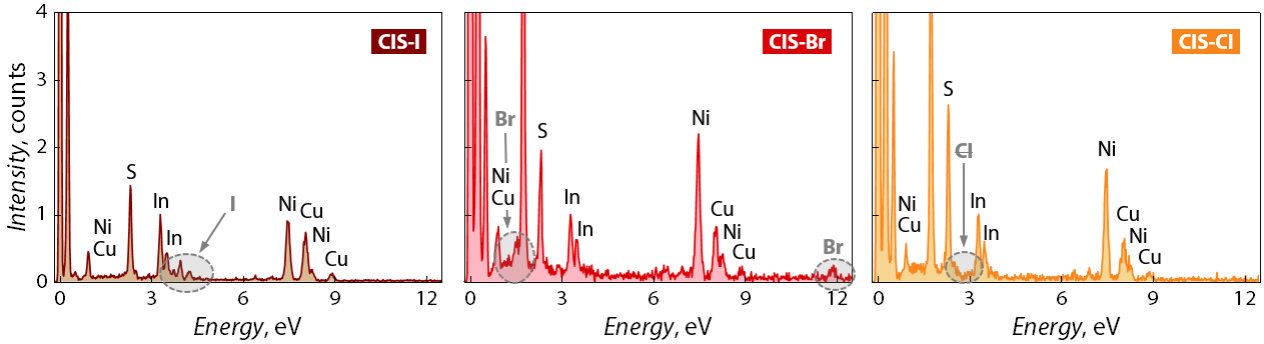

Figure S3. Results of the EDS analysis carried out during the TEM observations on the three samples CIS-I, CIS-Br and CIS-Cl reacted for 120 min.

Results of Rietveld refinements.

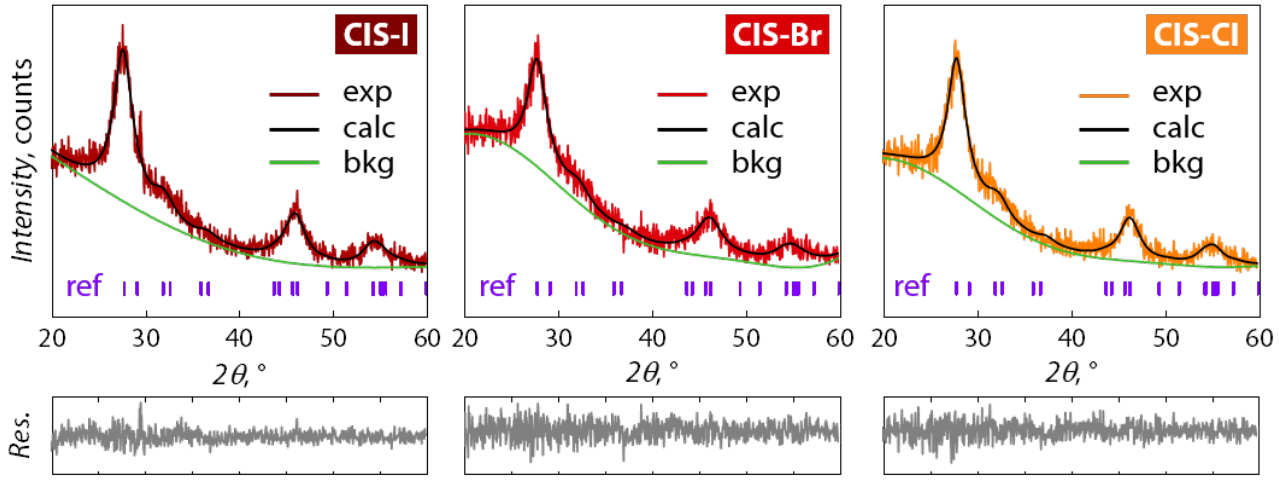

Figure S4. Rietveld refinements performed on the diffraction patterns of the three samples CIS-I, CIS-Br and CIS-Cl reacted for 120 min. The experimental data are plotted as solid colour-coded lines (burgundy – CIS-I; red – CIS-Br; orange – CIS-Cl). The calculated pattern and background are plotted as black and green solid lines, respectively. The position of the reference reflections for chalcopyrite $CuInS_2$ is indicated with violet tick marks. Residuals [*(exp-calc)/sigma*] are plotted as grey solid lines.

Additional XPS results.

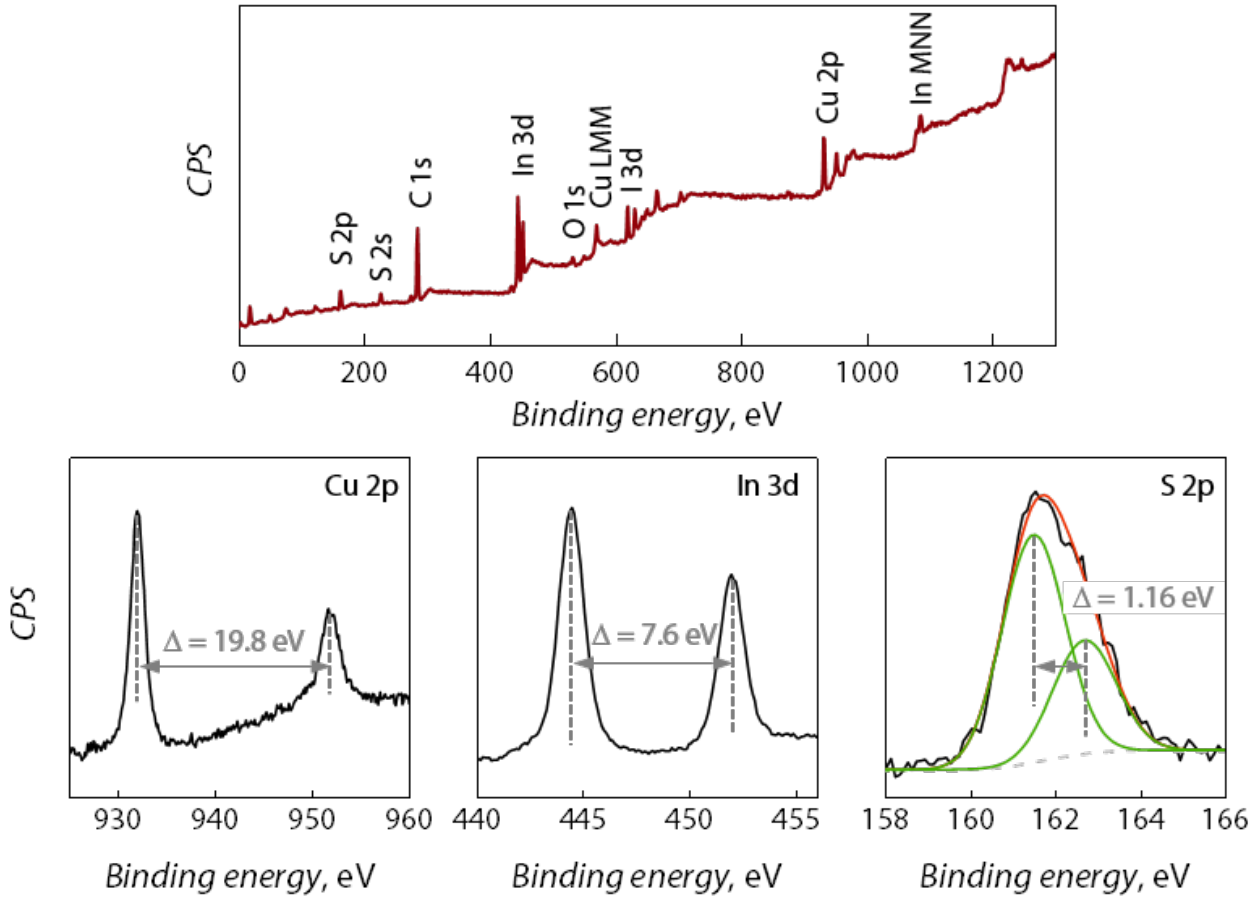

Figure S5. Survey (top) and Cu 2p, In 3d, S 2p high-resolution XPS spectra (bottom) recorded from the sample CIS-I reacted for 120 min.

Table S1. Attribution of the XPS signals for the samples CIS-I.

	***Calibrated BE*, eV**	***Assignment***
C 1s	284.4	Graphitic/adventitious carbon
O 1s	531.35	C=O
I 3d	619.9	Metal iodide
Cu 2p	932.0	Cu(I), possibly Cu-S or Cu-I. Since no characteristic weak satellite were observed, Cu(I)O is excluded
In 3d	444.5	In_2O_3, $CuInS_2$ or In_2S_3. Since no metal oxide peak were observed in O 1s, In_2O_3 is excluded
S 2p	161.55	Metal sulphide

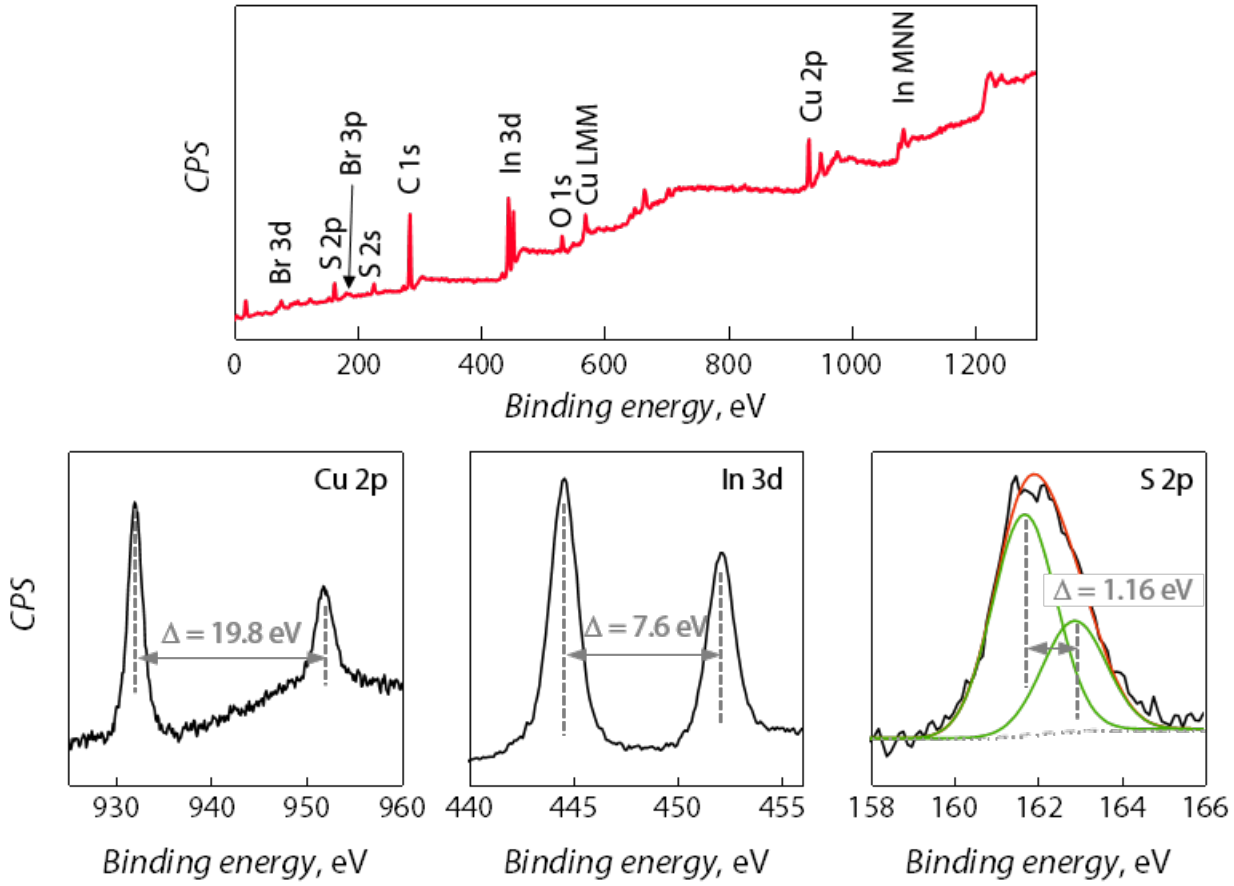

Figure S6. Survey (top) and Cu 2p, In 3d, S 2p high-resolution XPS spectra (bottom) recorded from the sample CIS-Br reacted for 120 min.

Table S2. Attribution of the XPS signals for the samples CIS-Br.

	***Calibrated BE*, eV**	***Assignment***
C 1s	284.4	Graphitic/adventitious carbon
O 1s	531.8	C=O
Br 3d	68.45 *74.25**	Metal bromide *Cu 3p peak**
Br 3p	182.05	Metal bromide
Cu 2p	932.05	Cu(I), possibly Cu-S or Cu-Br. Since no characteristic weak satellite were observed, Cu(I)O is excluded
In 3d	444.55	In_2O_3, $CuInS_2$ or In_2S_3. Since no metal oxide peak were observed in O 1s, In_2O_3 is excluded
S 2p	161.7	Metal sulphide

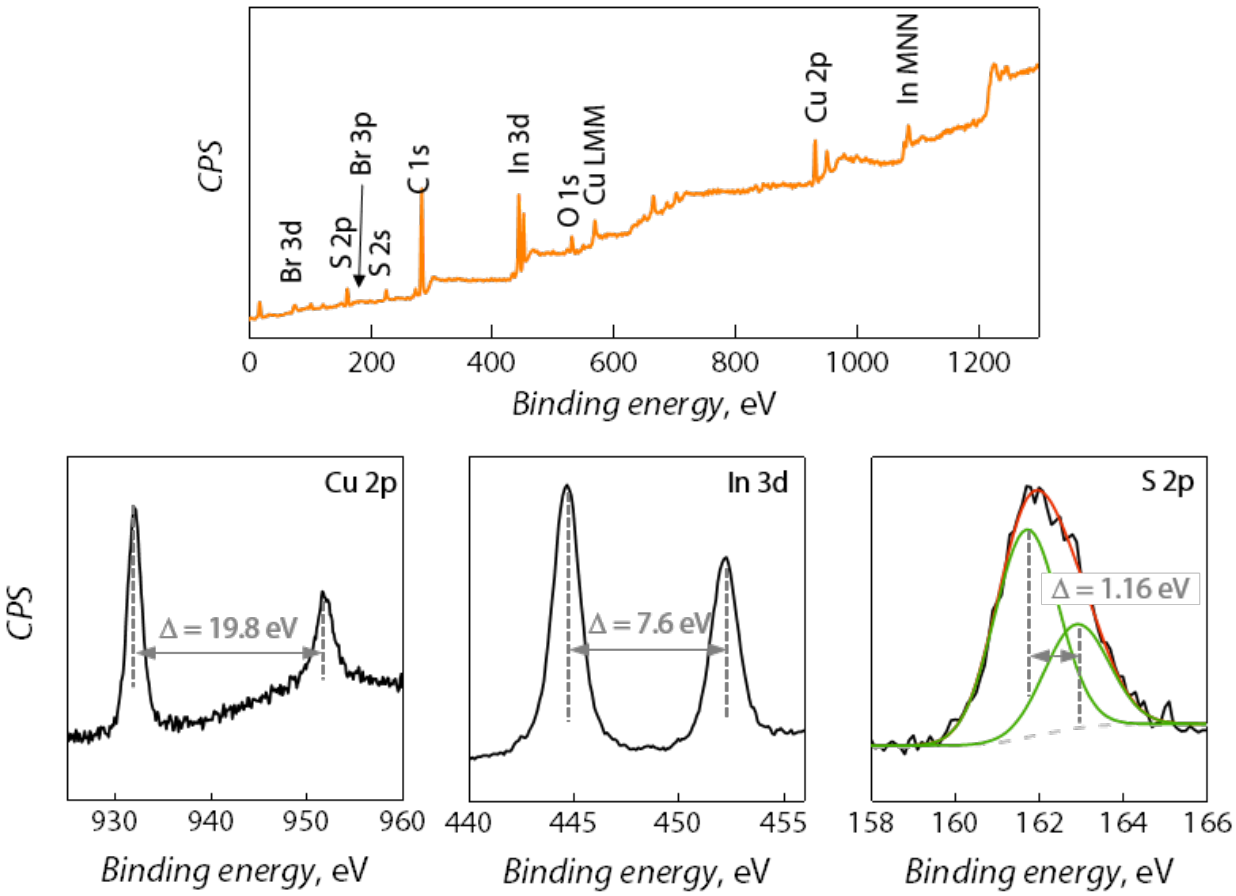

Figure S7. Survey (top) and Cu 2p, In 3d, S 2p high-resolution XPS spectra (bottom) recorded from the sample CIS-Cl reacted for 120 min.

Table S3. Attribution of the XPS signals for the samples CIS-Cl.

	***Calibrated BE*, eV**	***Assignment***
C 1s	284.4	Graphitic/adventitious carbon
O 1s	531.8	C=O
Cl 2p	198.4	Metal chloride
Cu 2p	932.0	Cu(I), possibly Cu-S or Cu-Cl. Since no characteristic weak satellite were observed, Cu(I)O is excluded
In 3d	444.55	In_2O_3, $CuInS_2$ or In_2S_3. Since no metal oxide peak were observed in O 1s, In_2O_3 is excluded
S 2p	161.6	Metal sulphide

Additional XAS results.

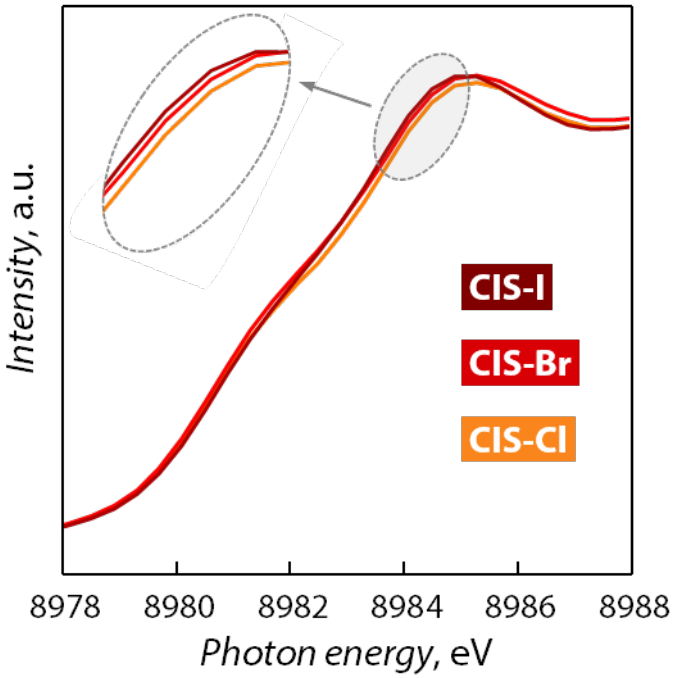

Figure S8. Close-up of the main peak of the Cu K-edge XANES spectra of the three samples reacted for 120 min. The zoom-in highlights the shift to lower energy of the main feature in the spectrum of CIS-I.

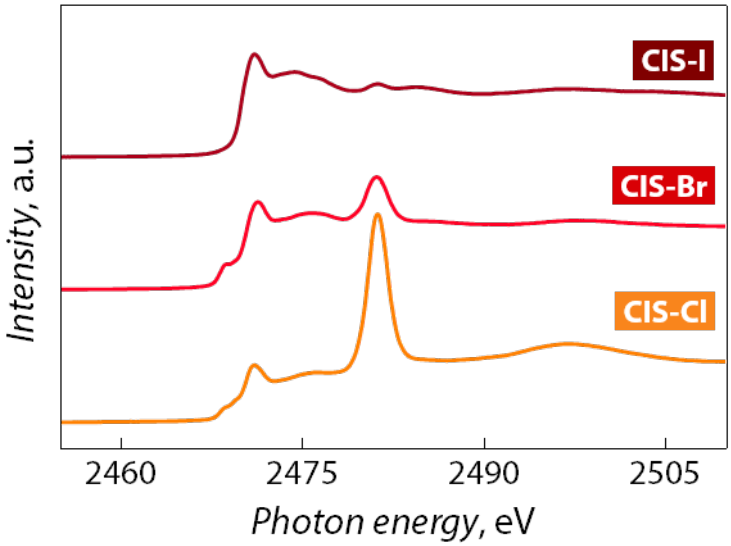

Figure S9. S K-edge XANES spectra of the three samples reacted for 120 min.

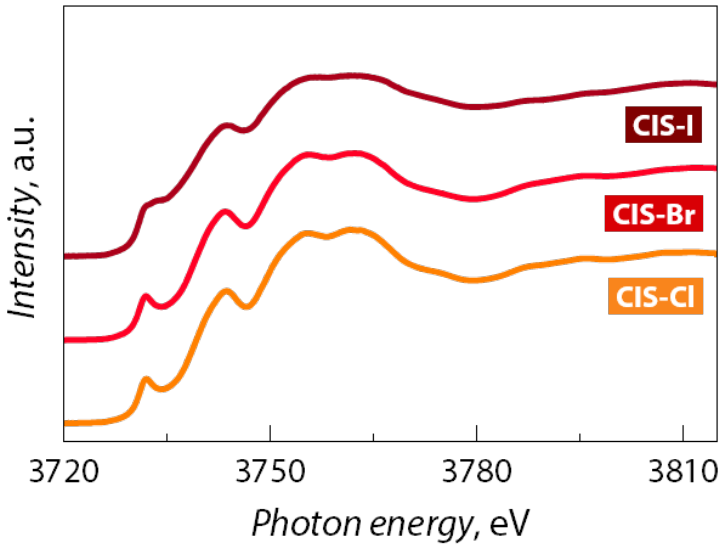

Figure S10. In L_3-edge XANES spectra of the three samples reacted for 120 min.

Additional photophysical characterization.

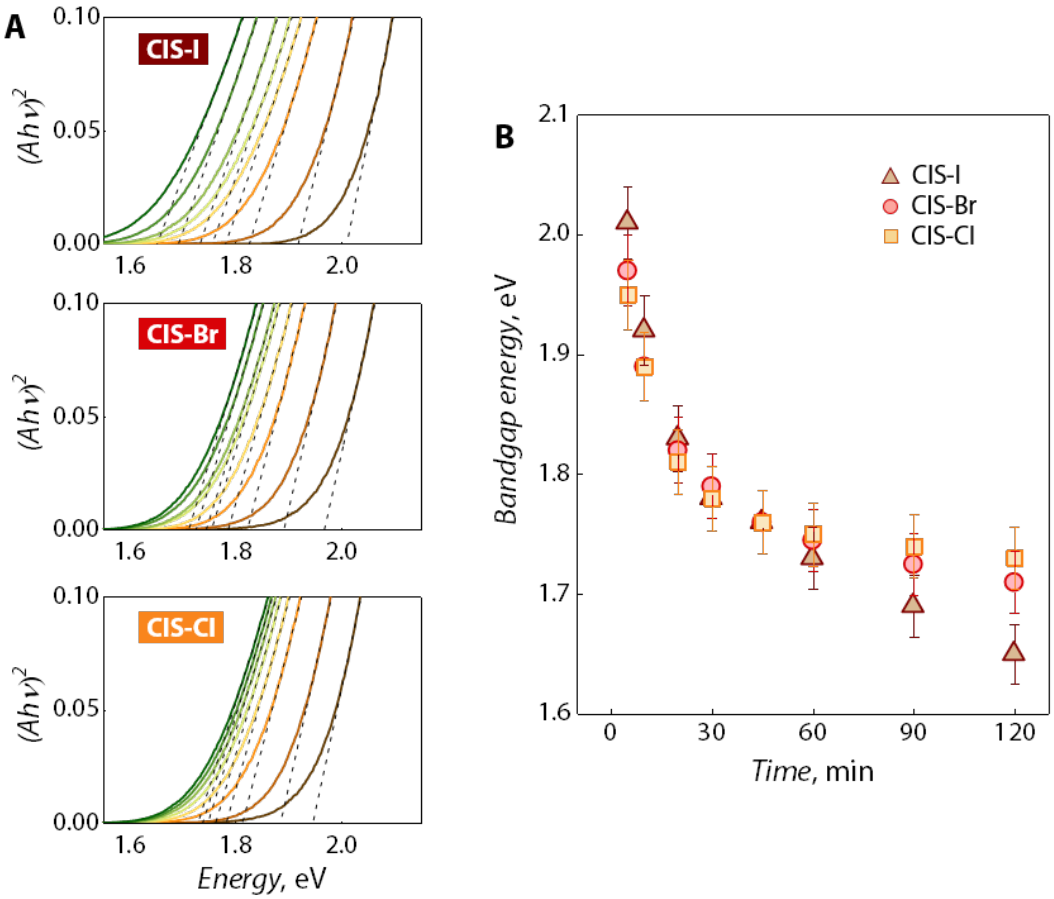

Figure S11. Tauc plots (A) derived from the absorption spectra reported in Figure 4A in the main manuscript. For these plots, since CIS is a direct bandgap material, $(Ahv)^2$ was plotted versus the photon energy hv (A is the absorbance, h is the Planck's constant, and v is the photon frequency). The linear part of the plot was extrapolated to $Ahv = 0$, and the intersection with the x-axis returned the bandgap energy (E_g). These extrapolated values are reported in B for all the samples.

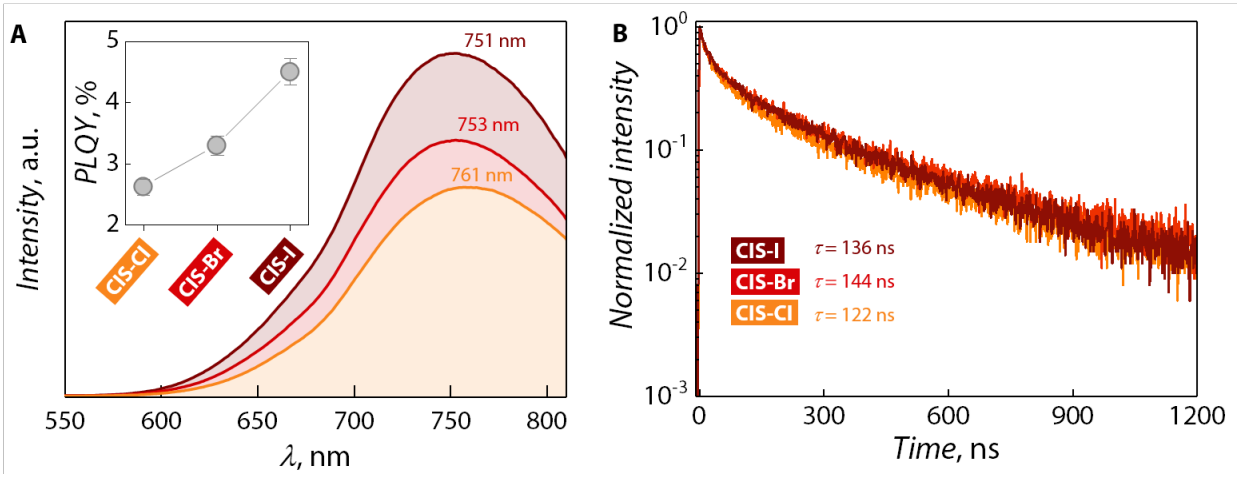

Figure S12. PL spectra (A) and decay curves (B) recorded from the aliquots of the three samples (CIS-Cl, CIS-Br, CIS-I) reacted for 30 min. The emission peak maxima and the average lifetime values are reported for each QD batch in A and B, respectively. In the inset in A, the *PLQY* values for each of the three samples are also reported. Errors on the *PLQY* values were estimated considering the uncertainty on the *PLQY* of the used standard: $Ru(bpy)_3Cl_2$ *PLQY* = (0.042 ± 0.002).[2]

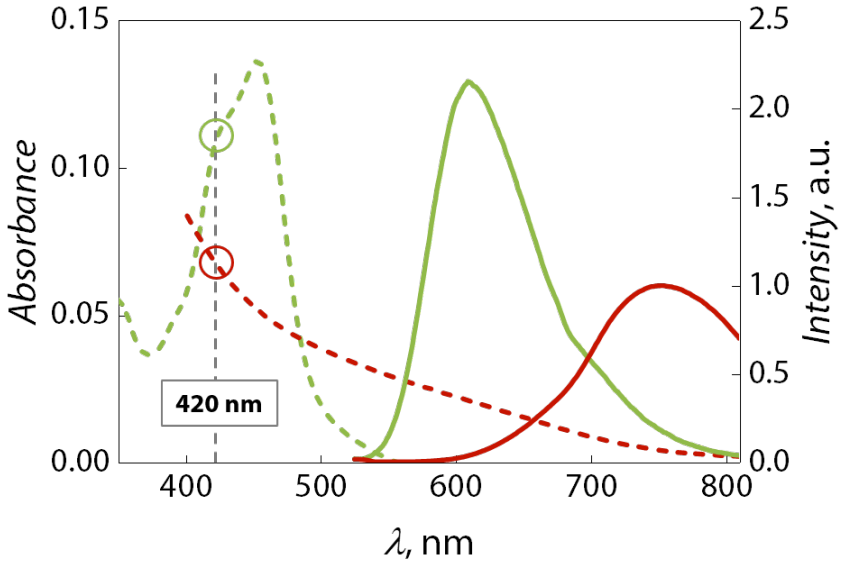

Figure S13. Dataset employed for the calculation of the *PLQY* values reported in Figure S12A. Optical extinction spectra (dashed lines) and emission spectra obtained under 420 nm excitation (solid lines) for CIS-I reacted for 30 min (red) and $Ru(bpy)_3Cl_2$ (green) are plotted. Circles in the extinction spectra highlight the OD values at 420 nm. The relatively good overlap between the extinction and emission spectra of the sample and the standard makes $Ru(bpy)_3Cl_2$ a suitable choice for the calculation of the *PLQY* of these QDs.

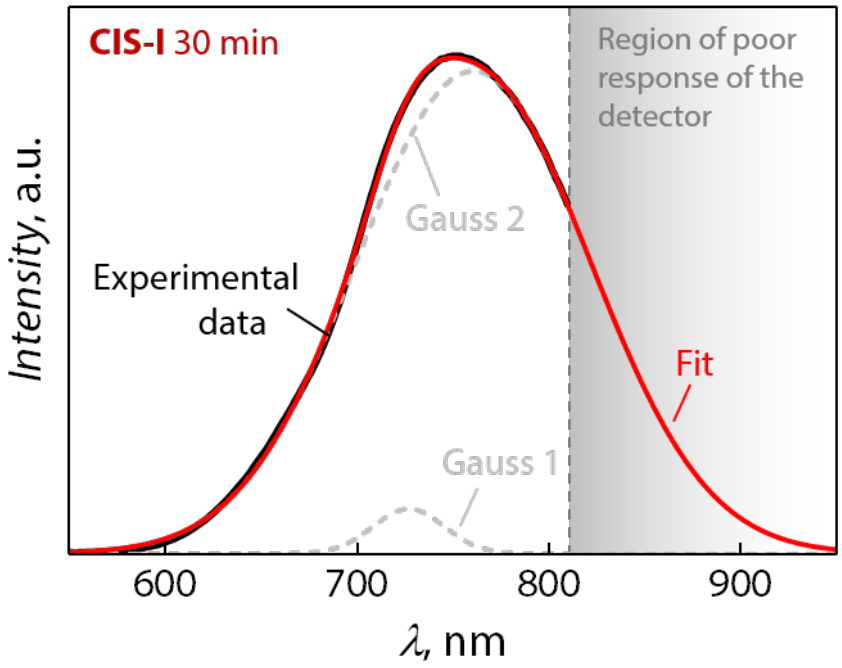

Figure S14. Typical fit procedure executed on the emission profile of the QDs obtained after 30 min of reaction using 2 Gaussian contributions (the case of CIS-I is presented). Using this approach, it was possible to roughly estimate the emission intensity in the wavelength region where the detector showed poor response – hence impeding recording the long-wavelength side of the QD emission. This procedure, although not accurate, allows treating the data equally for the three QD batches (CIS-I, CIS-Br, CIS-Cl) reacted for 30 min, thus retrieving a fair estimate of the relative emission efficiencies of these samples. Note that following this approach, the calculated *PLQY* is likely an underestimation of the real value, since often $CuInS_2$-based QDs feature asymmetric emission profiles with longer "tails" in the long-wavelength range.

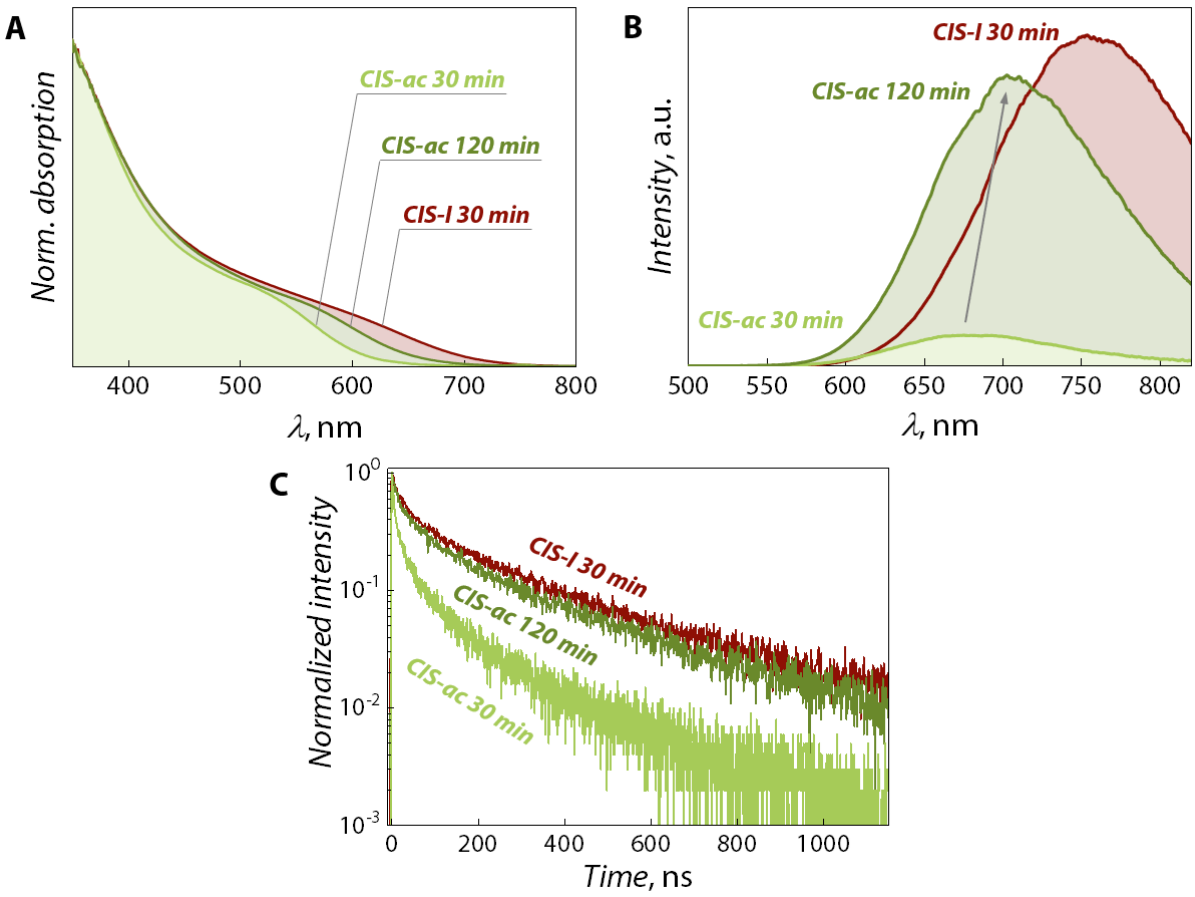

Figure S15. Comparison of the optical properties of a newly prepared batch of CIS-I reacted for 30 min and CIS QDs synthesized using copper acetate (CIS-ac) and reacted for 30 and 120 min. The blue-shifted absorption edge (A) and emission peak maximum (B) observed for CIS-ac compared to CIS-I suggests that the QD growth in the presence of acetate molecules is slower. This observation was further corroborated by the faster decay rate featured by CIS-ac QDs even after 120 min of growth compared to CIS-I QDs grown for only 30 min (C). Overall, these results signify the importance in choosing the specific metal precursors. Faster QD growth (being energetically favourable) can be obtained preferring metal salts to metal complexes. The emission spectra were recorded from colloids whose optical density at the excitation wavelength (455 nm in this case) was adjusted to 0.1, allowing for a reasonable comparison of the emission intensity featured by the three samples.

References

1. R. Marin, A. Vivian, A. Skripka, A. Migliori, V. Morandi, F. Enrichi, F. Vetrone, C. Aprile and P. Canton Mercaptosilane-Passivated $CuInS_2$ Quantum Dots for Luminescence Thermometry and Luminescent Labels *ACS Appl. Nano Mater.* **2019**, *2*, 2426-2436.
2. K. Suzuki, A. Kobayashi, S. Kaneko, K. Takehira, T. Yoshihara, H. Ishida, Y. Shiina, S. Oishi, S. Tobita Reevaluation of Absolute Luminescence Quantum Yields of Standard Solutions Using a Spectrometer with an Integrating Sphere and a Back-Thinned CCD Detector. *Phys. Chem. Chem. Phys.* **2009,** *11*, 9850-9860.